Experimental Investigation of Reverse Fault Rupture – Rigid Shallow Foundation Interaction

S. M. Moosavi[1], M. K. Jafari[1], M. Kamalian[1] and A. Shafiee[1]

Received: November 2009 Accepted: April 2010

Abstract: *Ground differential movements due to faulting have been observed to cause damage to engineered structures and facilities. Although surface fault rupture is not a new problem, there are only a few building codes in the world containing some type of provisions for reducing the risks. Fault setbacks or avoidance of construction in the proximity to seismically active faults, are usually supposed as the first priority. In this paper, based on some 1-g physical modelling tests, clear perspectives of surface fault rupture propagation and its interaction with shallow rigid foundations are presented. It is observed that the surface fault rupture could be diverted by massive structures seated on thick soil deposits. Where possible the fault has been deviated by the presence of the rigid foundation, which remained undisturbed on the footwall. It is shown that the setback provision does not give generally enough assurance that future faulting would not threaten the existing structures.*

Keywords: *reverse fault rupture, interaction, rigid shallow foundation*

1. Introduction

Ground differential movements due to faulting were highlighted dramatically as a significant hazard affecting engineered structures and facilities after recent earthquakes in Turkey and Taiwan in 1999 [1,2,3]. In these events, a large number and a wide variety of structures were subjected to tectonic displacements ranging from 2 to 8 m. Along with the often-spectacular observations of damages documented by these recent events, examples of satisfactory performances of structures emerged, too. These examples confirmed this view point that structures could also be designed to withstand large ground differential movements due to fault ruptures [4,1].

Different approaches have been adopted to investigate the surface fault rupture hazard such as field studies [5,6,7,8,9 ,4], physical modeling [10,11,5,12,13,14], numerical modeling [15,16] and analytical approaches [17,18].

Considerable effort in the above mentioned studies has been devoted to determine the location of the surface fault rupture as well as the width of the affected zone in alluvium over dip slip faults. The reason is that fault setbacks or avoidance of construction in the proximity to seismically active faults, were usually supposed as the first priority by building codes and regulations. For instance, the well known Alquist-Priolo Earthquake Fault Zoning Act of the California State proposed a setback of around 50ft (15.3m) from each side of the fault trace, whereas the Iranian and the European seismic codes forbade any construction within the "immediate vicinity" of active fault traces.

It is obvious that with increasing demands on land use, avoidance is becoming more difficult. In addition, the exact position of a fault trace and especially those of its sub-faults are often difficult to locate with an acceptable precision. Further, the fault rupture propagation through surface layers in the presence of existent structures does not seem to be necessarily the same as in their absence. i.e. in the free field case. Therefore it seems still logical as well as necessary to pay much more attention in order to get a better understanding of the surface fault rupture propagation pattern and its interaction with shallow foundations in order to reduce damage or collapse of the structures.

This paper presents some clear perspectives of surface reverse fault rupture propagation and its interaction with shallow rigid foundations seated on thick soil deposits, obtained by simple 1-g

* *Corresponding author. Email: jafari@iiees.ac.ir*

1 Geotechnical Engineering Research Center, International Institute of Earthquake Engineering and Seismology (IIEES), Tehran, Iran.

physical modeling tests. The tests were concentrated on reverse faults, because of the practical importance of this kind of faults in Iran. It is well known that the Iranian plateau accommodates the 35 mm/yr convergence rate between the Eurasian and Arabian plates by mostly reverse faults with relatively low slip rates in a zone 1000 km across [19,20]. Assessing clear answers to the following two questions constituted the main essences of this paper:

1. Could existing structures deviate the future surface fault rupture pattern?
2. Could the well known concept of 50 feet fault setback give enough assurance that future faulting would not threaten the existing structures?

2. Physical Modeling Methods

A review on the relevant literature reveals that many physical modeling tests have been made during the last decades in order to get a more realistic understanding of the fault rupture propagation pattern throughout the surface soil layers. These physical modeling tests constituted of either the 1-g physical model tests, which were performed just under the normal gravity conditions [10,12] or the centrifuge tests, which were executed under some kind of accelerated gravity conditions [11,13].

Stone and Wood (1992) carried out some 1-g model tests as well as some centrifuge tests in order to compare the observed rupture propagation patterns in a sand layer subjected to vertical normal faulting. The box in which the tests were carried possessed a trapdoor. The models, which contained lead shots at different locations, were analyzed with radiographic techniques after faulting. The comparison indicated that (Fig 1):

- The rupture patterns under 1g and 100g were somewhat similar.
- The level of confinement might not be the primary factor that controls the rupture pattern. Instead, the dominant factor that controls the strain localization direction, was the kinematics constraint due to the angle of dilation, mobilized within the zone of localization.
- Although the rupture patterns due to the two levels of gravity were somewhat

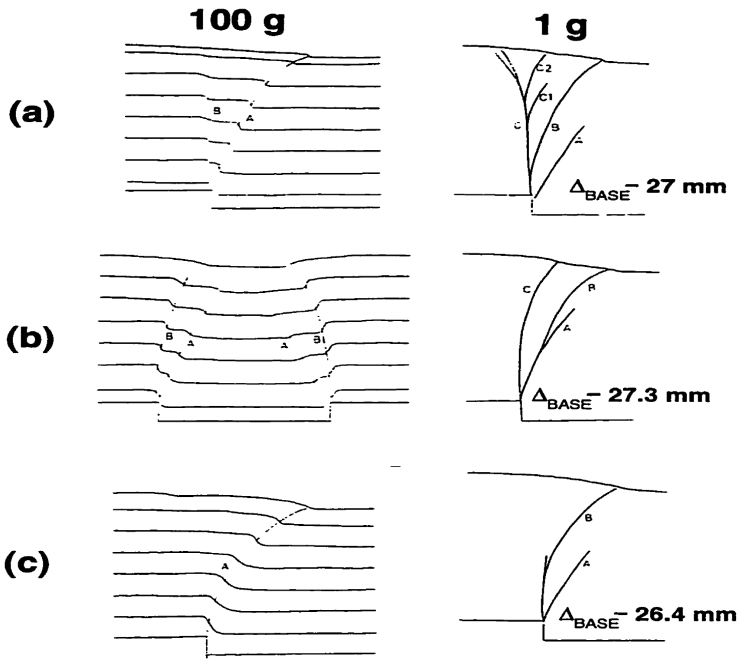

Fig. 1. Comparison of the final rupture pattern of sand models under 100g and 1g after a vertical normal fault movement of around 25mm for: (a) D50= 0.4mm,(b)D50= 0.85mm, and (c) D50= 1.50mm; A,B,C: order of crack occurrence (Lazarte,1996 taken from Stone,1988)

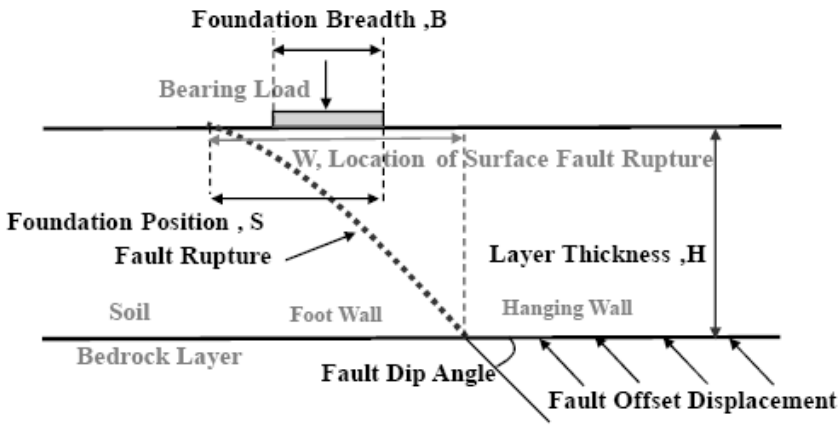

Fig.2. Geometry of reverse fault rupture emergence adjacent to a shallow foundation

comparable, but they did differ by the number of ruptures. In the 1-g model tests, in which case the initially dense sand would be significantly more dilative than in the 100-g case, more ruptures were observed.

Stone and Wood (1992) also noticed that the ratio of base displacement to the grain size is an important factor that affects the rupture pattern. In the case of sand layers with equal thicknesses, similar rupture patterns were observed when the base movement to the grain size ratio was the same.

Tani et al. (1996) executed some 1-g model tests where a 90 degree fault sheared the sand layer for about 5 to 200 cm. They noticed that the fault rupture pattern was affected by the thickness of the layer. They noticed as well that the amount of the base offset required for propagation of the shear zone to the ground surface, depended in a non-linear manner on the layer thickness.

Sand layers with a thickness of about 40cm or more required a smaller normalized base offset to height in order to enable the fault rupture to reach the ground surface. The thickness of the sand layer also affected some other aspects of the rupture pattern. For example, fewer ruptures were observed in sand layers with a thickness of less than 20cm. In addition, the shear pattern in larger models was typically more complex than in shallow models.

The above mentioned observations showed that there exists a "scale effect" in 1-g model tests which could not be disregarded. Tani et al. (1996) argued that when the same sand is used in various tests with different layer thicknesses, the particle size would not be scaled by the same geometrical scale. In other words the fault rupture patterns were somewhat different, where the ratio of the layer thickness to the grain size was not the same. However these investigators noticed that this scale effect affected the test results only in those models that had a layer thickness to grain size ratio smaller than a threshold size. For sand layers with a thickness to grain size ratio larger than this threshold size, the observed fault rupture patterns were comparable and approximately the same.

Lee and Hamada (2005) observed that while in 1-g model tests with a sand layer thickness of more than 20cm several rupture planes could be seen, in the centrifuge model tests only a continuous rupture plane was observed throughout the entire sand layer. They also observed that in 1-g small scale sandbox model tests, increasing the sand layer thickness (H) resulted in a slight decrease in the W/H ratio, where W denotes the location of the fault trace on the ground surface (Fig.2). But in centrifuge tests, no definite relation was found between the sand layer thickness and the location of the fault trace on the ground surface. This implied once again the importance of this fact that in order to estimate the location of the fault trace on the ground surface by 1-g small scale sandbox model tests, particular caution should be paid to the important possible effect of the dry sand dilation angle at extremely low confinement on the rupture pattern. In other words, the fault rupture propagation pattern through a sand deposit was found to be obviously affected by its confining stress level.

3. Apparatus and Test Program

The present study was mainly intended to study the interaction of shallow rigid foundations with the typical generic geometry macrostructure patterns of reverse fault surface rupture propagation (Fig. 2).

Based upon the in literature registered experimental works reviewed in the previous section, it may be concluded that 1-g model tests could be reliable for the investigation of fault rupture foundation interaction. Because, according to Stone and Wood (1992), the macrostructure fault rupture propagation pattern would be similar in 1-g model and centrifuge tests, regardless of the gravity conditions. In addition, according to Tani et al. (1996), the scale effect on tests at normal gravity conditions, seems to disappear in models larger than a threshold model size, which could be defined as 20 cm based on Lee and Hamada (2005). In addition, the model size of 20cm generates a continuous rupture plane over the entire thickness of model similar centrifuge models.

Hence, the 1-g physical modeling approach was adopted in the present study, particularly since the 1-g model tests were much more economic and accessible. The device used for performing the 1-g model tests were designed in such a way that reverse as well as normal fault rupture events could be modeled along different dip angles. Two plexiglass plates were provided at each side of the box and perpendicular to the fault strike, in order to enable digital photography of the vertical section throughout the soil. The executed tests investigated reverse fault rupture propagation with a dip angle of 45 degree through the bedrock in a quasi- static mode using an electric motor.

The sand used in the present study was the well known Firoozkooh sand (No.161), which is commercially available from the Firoozkooh mine in north east of Tehran. It has a uniformly graded (SP) size distribution as well as a mean grain size (D_{50}) of 0.25 mm. The sand layer had a length, width and thickness of 100, 40 and 20 cm, respectively, which modeled the plane strain condition approximately. The pluviation technique with a pre-defined height and velocity of a designed hopper was used to fill the box with a relative density of approximately 85%.

A steel block, with a width (B) of 50 mm, a height of 10mm and a length of 40 mm, was placed on the top surface of the soil in order to represent the rigid shallow footing. So, as the sand layer had a thickness (H) of 20cm, the H/B ratio was equal to 4 in all 1-g model tests of the present study.

In total, 9 1-g model tests were performed by varying the most important geometrical parameters introduced in Fig.2. The first test was conducted in the absence of the footing, in order to locate the fault trace on the ground surface under the free field conditions. The next tests were conducted in the presence of the footing. Each time, the footing's distance to the free field fault trace as well as its bearing pressure was changed.

Table 1 categorizes the conducted tests in 3 different groups based on the bearing pressure in order to simplify the further explanation of the test results. The medium bearing pressure will be presented firstly in the next section as a reference loading on soil surface and then the lighter and heavier bearing pressures will be studied.

Table 1. Model tests conditions

Test No.	Bearing Pressure (kPa)	Foundation Position (S/B)	Category
1	Free Field	-	-
2	3.75	1	Medium
3	3.75	2	Medium
4	3.75	3	Medium
5	3.75	4	Medium
6	1.25	1	Light
7	1.25	2	Light
8	8.75	3	Heavy
9	8.75	4	Heavy

4. Test Results

4. 1. Free Field Condition

The experiment investigating the propagation of a reverse fault through soil in absence of a footing ("free field "test) was conducted first to find where the free field fault would emerge at

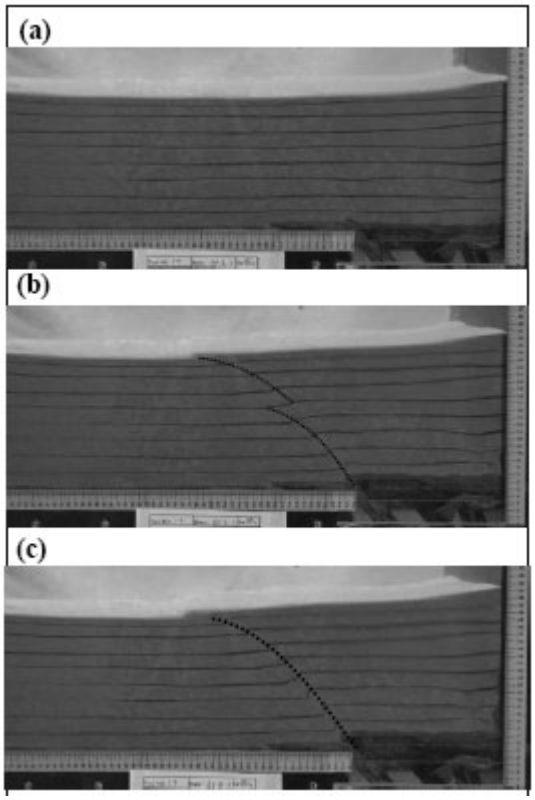

Fig. 3. reverse fault (45 degree dip angle) rupture propagation in free field condition (1-g condition) at three stages (a) without base dislocation,(b)small base dislocation (c)final mechanism

the ground surface. The test result was further used to locate the foundation position in the foregoing tests and examination of fault rupture pattern modification due to foundation. The images captured at three stages of the fault displacement are shown in Fig. 3.

Small fault displacements produced a gradual distortion toward the soil surface and a first localization was visible near the bedrock discontinuity. The fault propagation is progressive and following fault displacement (Fig. 3b), two shear planes are developed through the soil layer, near the base and the soil surface with evident fault trace at the ground surface. As the final mechanism is generated on large fault displacement (Fig.3c) an inclined zone of large shear deformation, with an average dip angle of 40 degrees, is formed running from the bedrock to the surface with a visible displacement discontinuity on the soil surface.

Therefore, the fault dip angle reduces as the soil surface is approached and the fault trace

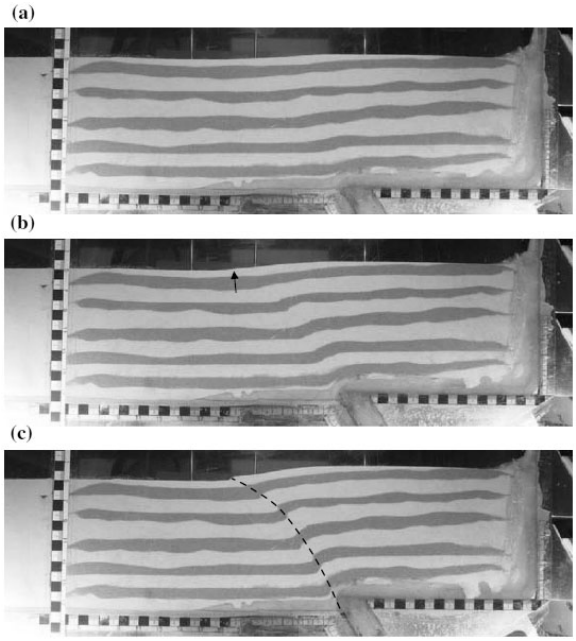

Fig. 4. Free-field reverse faulting (60 degree dip angle) rupture propagation in 3 stages in centrifuge condition (Bransby et al., 2008)

emerges on the soil surface. Soil to the left side of the fault (on the foot wall side of the fault) appears relatively undisturbed; whereas the soil on the right side of the fault (on the hanging wall side of the fault) has been distorted by fault propagation.

Examination of the sequence of the digital images captured during the simulated faulting event in the case of performed studies herein agree very well with centrifuge test results as presented by Bransby et al., (2008) (Fig. 4). The same global pattern was observed in 1g and centrifuge testing.

4. 2. Fault – Foundation Interaction in Medium Bearing Pressure State

Four foundation tests in different positions were conducted in medium bearing pressure state with the same soil conditions as for the free-field test, with the foundation width B=5cm and bearing pressure of q=3.75kPa.

In the first foundation test in this group (No.2), the footing was positioned in the vicinity of the free–field fault rupture, i.e. S/B=1, (Fig. 5a). As shown in Fig. 5b, a continuous localization (fault) in soil could be observed from the base

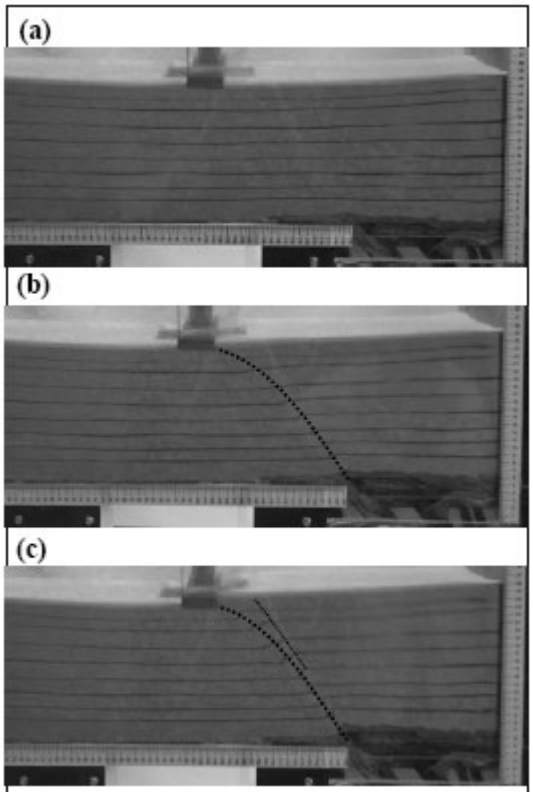

Fig. 5. reverse fault (45 degree dip angle) rupture propagation with medium foundation (S/B=1)

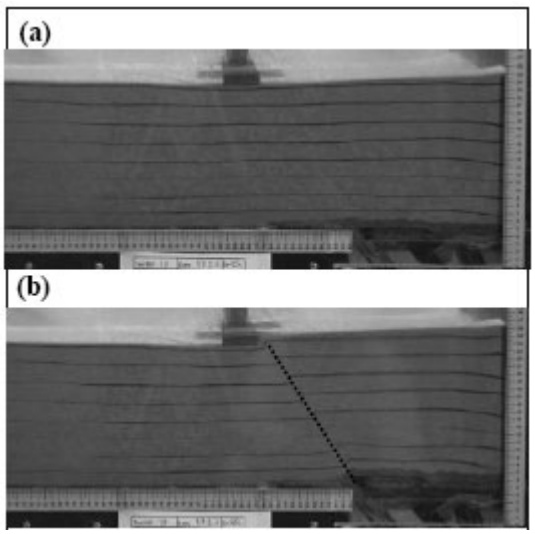

Fig. 6. Reverse fault (45 degree dip angle) rupture propagation with medium foundation(S/B=2)

discontinuity to the nearest (right hand) edge of the footing affected by the fault foundation interaction. The emergence position of the new fault has been deviated about 5cm from the free

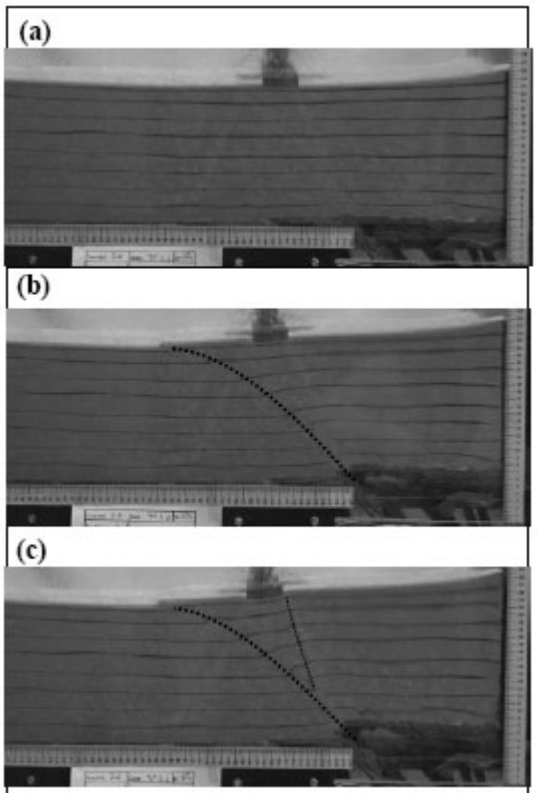

Fig. 7. reverse fault (45 degree dip angle) rupture propagation with medium foundation(S/B=3)

field condition towards the hanging wall side, protecting the foundation from significant rotation. It is interesting to note that by increasing the fault displacement (Fig. 5c), a second rupture would also be generated in the top surface layer and right to the main one, with no effect on the foundation.

In the second foundation test in this group (No.3), the foundation position has been changed to the S/B=2 as shown in Fig. 6a. Similar to pervious test in this group, a continuous localization (fault) is generated from the base discontinuity to the nearest (right hand) edge of the foundation (Fig. 6b) without significant movement imposed on foundation. One difference is that no second rupture developed further continuing the fault displacement.

The results of the third foundation test in this group (No.4) with S/B=3 (Fig. 7a) are very different from two previous ones. Significant foundation rotation and slip as well as two strong localizations occur in this test. The main strong localization (Fig. 7b) was first mobilized at fault displacement in bedrock, with dip angle

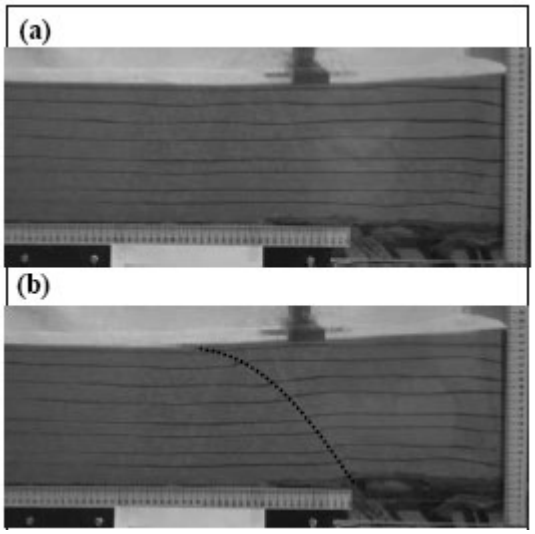

Fig. 8. reverse fault (45 degree dip angle) rupture propagation with medium foundation(S/B=4)

reduction in approaching the soil surface. The fault rupture emergence was occurred, in this case, at about 19cm from the left hand side of the foundation with approximately 9cm deviation to the foot wall side comparing to free field condition. The 2nd localization (Fig. 7c) was also generated in soil layer on further fault displacement. Although, the 2nd faulting emerges at the right corner side of the foundation; more rotation is imposed on the foundation. These aspects of behavior could likely damage a real foundation significantly.

Finally, in the forth foundation test in this group (No.5) with S/B=4 (Fig. 8a), the obtained results are similar to pervious test in this group (No.4) but without any secondary localization. The fault rupture emerges at the left hand side of the footing at about 21cm from the far edge (Fig. 8b) with no significant risk on foundation.

4. 3. Fault – Foundation Interaction on Light Bearing Pressure State

Two foundation tests with similar positions (Fig. 9) to tests No. 2 &3 were conducted under 1.25 kPa bearing pressure in this group. The soil condition was the same as for the free-field test. In the first foundation test (test No.6), the results are similar to ones in medium bearing pressure state (test No. 2). As it is demonstrated in Fig. 9b, the fault emerges at the right corner of the

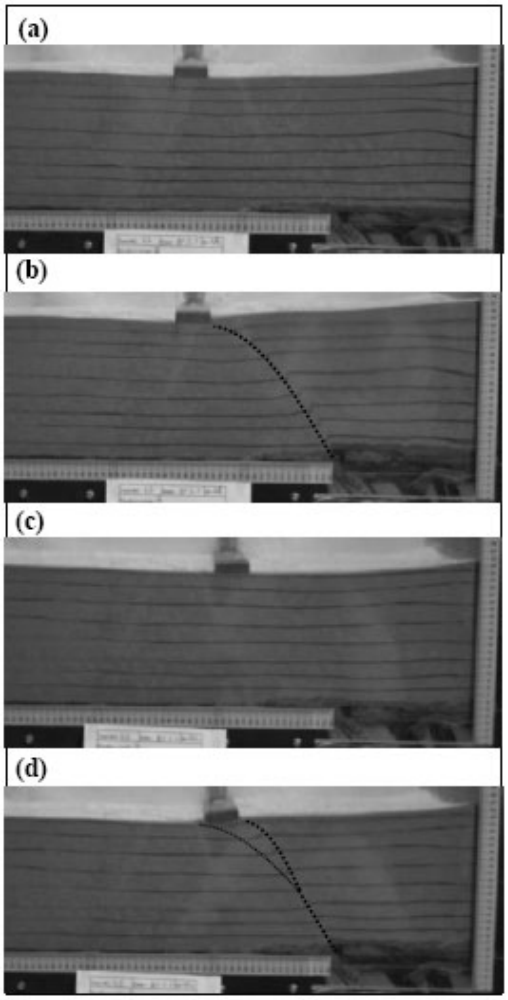

Fig. 9. reverse fault (45 degree dip angle) rupture propagation with light foundation (a and b with S/B=1, c and d with S/B=2)

foundation without any important imposed movement on it. Although, the results in the second foundation test in this group (test No.7) are similar to test No.4 (Fig. 9c), but they are different from the test No.3. The foundation undergoes small rotation and slip and two localization planes, with the stronger one in the right hand side (Fig. 9d), are developed in both sides of the foundation.

4. 4. Fault – Foundation Interaction on Heavy Bearing Pressure State

Two foundation tests with similar positions (Fig. 10) to tests No. 4&5 were also conducted under 8.75 kPa bearing pressure in this group. The soil condition was also the same as for the

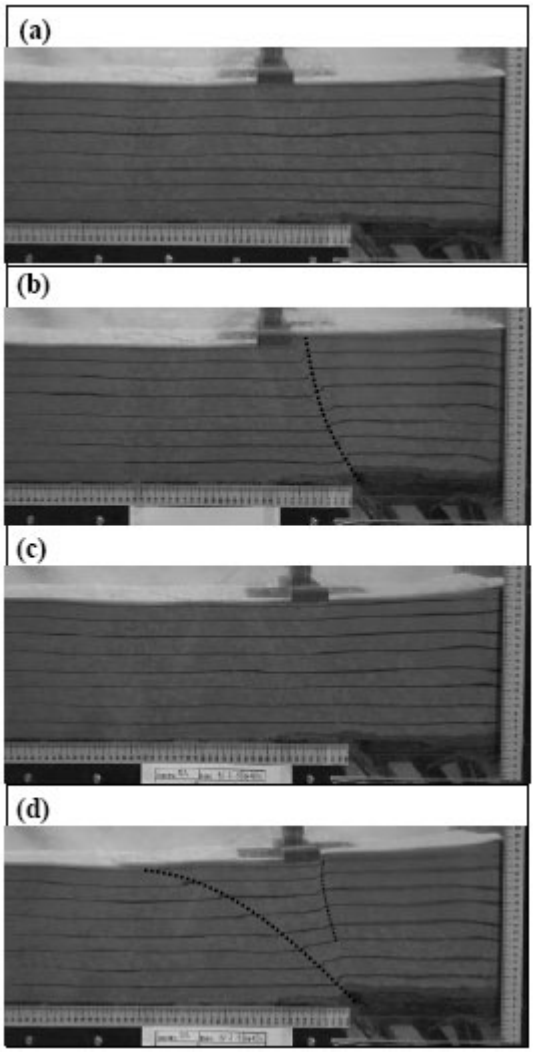

Fig. 10. reverse fault (45 degree dip angle) rupture propagation with heavy foundation (a and b with S/B=3, c and d with S/B=4)

free-field test. In the first foundation test (test No.8), the results are different to ones in medium bearing pressure state (test No. 4) but there are similarity with results in tests No. 2,3,6. As it could be seen in Fig. 10b, the fault emerges at the right hand side of the foundation without any imposed rotation on it. Although, the results in the second foundation test in this group (test No.9) are similar to test No.5 but some difference could also be observed. The fault rupture emerges at the left hand side of the foundation at about 31cm from the far edge (Fig. 10d). The 2nd localization was also generated in soil layer during fault displacement, emerging at the right hand side of the footing, without significant effect on the foundation.

5. Discussion

A clear summation of the reverse fault rupture propagation patterns observed during the 1g physical modeling tests performed in the present study is demonstrated in Fig.11. As can be seen, there were two main parameters that controlled the interaction of the fault rupture propagation and the rigid shallow foundations: the foundation's position and its bearing pressure. Where possible, the rigid foundation deviated the fault to its right side and remained undisturbed on the footwall. This behavior which could be easily justified by the well known principle of the minimum work, dominates the reverse fault rupture propagation, when the bearing pressure

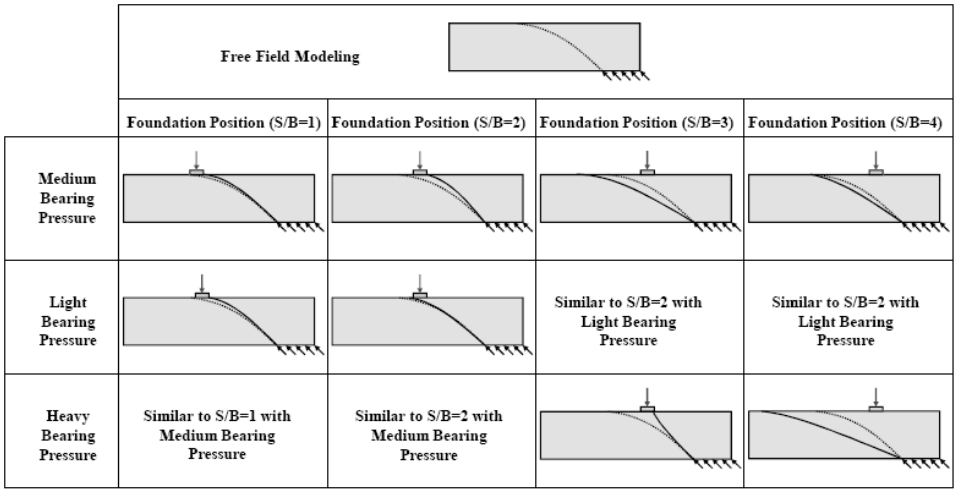

Fig. 11. the schematically results of the present investigation

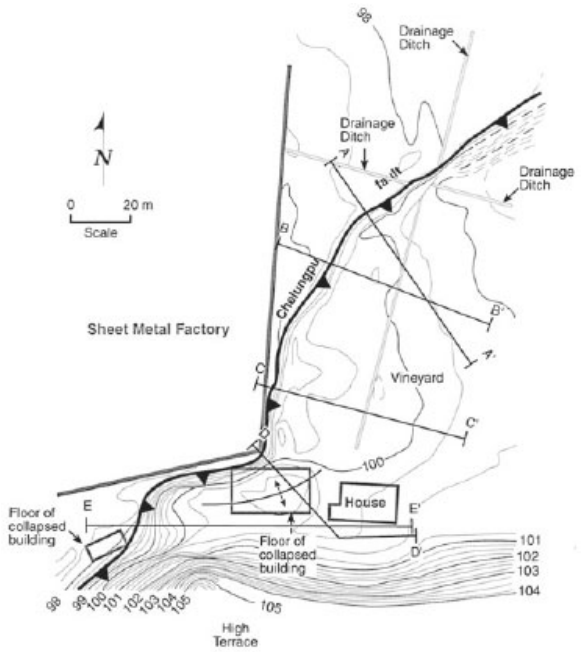

Fig. 12. Topographic map of the Experimental Vineyard site, showing Chelungpu fault scarp, topographic profile locations, and existing buildings. Contour interval = 25 cm. The foundation deviates the fault and the foundation is left almost undisturbed on the footwall (Kelson et al., 2001)

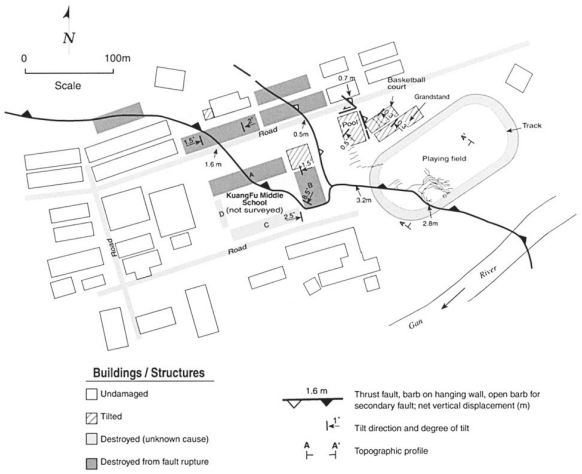

Fig. 13. Map of the Chelungpu fault at KuangFu Middle School, The foundation deviates the fault and remained entirely on the hanging wall of main fault strand (Kelson et al., 2001)

was heavy and the foundation was not located too far from the free field fault trace. Where not possible, the rigid foundation deviated the fault to its left side and was settled on the hanging wall. This behavior dominates the reverse fault rupture propagation, when the bearing pressure was light and the foundation was located too far from the free field fault trace. It should be mentioned that due to low value of B/H=0.25, the case of fault emergence beneath the foundation is not observed in this investigation and therefore herein in all discussions and conclusions this case was excluded.

In order to get deeper insights into the reverse fault rupture propagation pattern and its interaction with rigid shallow foundations, it seems valuable to compare the results obtained during the model tests of the current study with the field observations of well documented case histories as well as full scale numerical analysis.

- Field Observations

Since the Chi-Chi earthquake in 1999 generated substantial reverse fault rupturing at the ground surface, crossing numerous structures, and providing a great variety of real case histories of fault foundation interaction, this event can be claimed to comprise these reverse faulting-foundation interaction mechanisms here. Two main mechanisms were identified based on well-documented field cases [3] similar to physical modeling test results as follow:

- The foundation presence leads to deviation of the fault to its right side (Fig. 12) leaving the foundation almost undisturbed on the footwall. As shown in Fig.12 a massive sheet-metal factory on the footwall affected the form and location of the surface deformation. At this site, the scarp wraps around the southeastern corner of the building.
- The foundation deviates the fault to its left side where the foundation remained entirely on the hanging wall. As shown in Fig. 13, the main fault strand encounters building B and it bifurcates into a main strand, which passes under the building, and a secondary strand along the eastern wall of the building.

- Numerical Analysis

The well known Plaxis Software [21] based on the non-linear time-stepping finite element approach was used to carry out the numerical analysis. This kind of approach for verification of

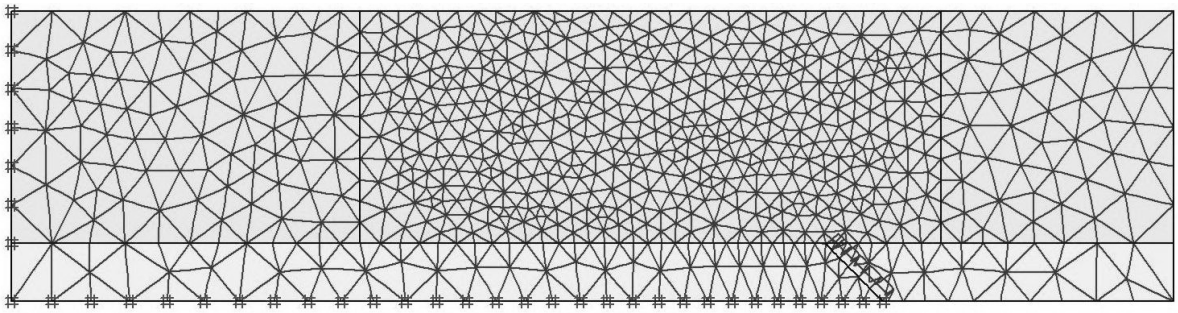

Fig. 14. A typical finite element mesh generated for the numerical analyses

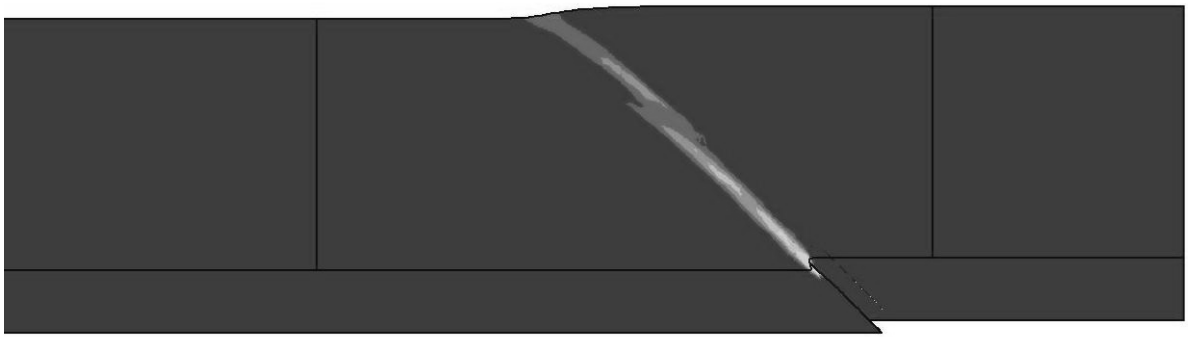

Fig. 15. Reverse fault (45 degree dip angle) rupture propagation in free field condition (FE deformed mesh with shear strain contours)

Fig. 16. Fault-foundation interaction with S/B=1 (FE deformed mesh with shear strain contours)

physical modeling tests are also used by the others [22,23]. In addition Mohr-Coulomb model with the following mechanical properties was used to simulate the elasto-plastic behavior of the soil:

- Friction Angle φ =37°
- Dilation Angle ψ =0 °
- Elastic Modulus E=675MPa
- Poisson's Ratio ν =0.35

The geometric dimensions of the numerical model were assumed to be 100 times greater than those of the physical model. The footing width (B) and the soil layer thickness (H) were selected as 5 and 20 meters, respectively. The numerical simulation of fault – foundation interaction model tests on light bearing pressure with bearing pressure of q=125kPa, are just selected for presentation in this paper. Interface elements similar to those used by Langen and Vermeer (1991) for analyses of trapdoor problems were used in order to model the onset of the rupture (Fig. 14). A rigid layer with a thickness of 5 meters was introduced beneath the soil layer in order to model bed rock. The static displacement

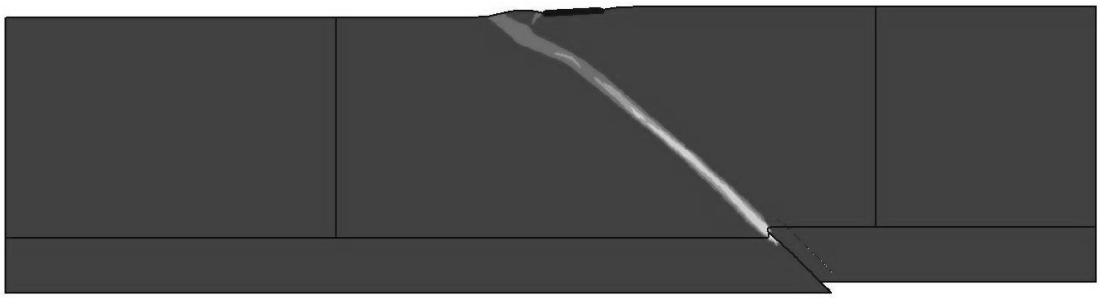

Fig. 17. Fault-foundation interaction with S/B=2 (FE deformed mesh with shear strain contours)

was imposed upwards at those boundary nodes lying at the right hand side of the fault rupture trace in order to simulate the reverse fault rupture trough the bed rock. A maximum value of 1 meter was imposed during a maximum number of 10000 loading steps.

The first runs of the numerical analysis were carried out in the absence of the foundation in order to locate the free field fault trace on the ground surface. Fig. 15 demonstrates the deformed geometry of the free field medium with the superimposed shear strain contours. The next runs were carried out in the presence of the foundation in order to model its impact on the fault rupture propagation. Figures 16 and 17 demonstrate the deformed geometries of the medium with the superimposed shear strain contours corresponding to two cases of (S/B = 1.0) and (S/B = 2.0), respectively. As can be seen, the numerical results confirm relatively well the main ideas observed in the physical modeling tests. In the case of (S/B =1), the rigid foundation could deviate the fault to its right side and remain undisturbed on the footwall, because it was not located too far from the free field fault trace. But in the case of (S/B =2), the rigid foundation could not deviate the fault to its right side and settled on the hanging wall, because it was located too far from the free field fault trace and its bearing pressure was light.

6. Implication for Design

Based on the observed interaction between the reverse fault propagation pattern and the rigid foundation, it seems that four distinct zones could be defined as follows around a free field reverse fault trace (Fig. 18):

- Zone 1, the footwall side of the free field reverse fault trace, where the surface displacement would be much smaller than to threat to the structure in future faulting.
- Zone 2, on the hanging wall and immediately adjacent to the free field reverse fault trace, where the fault propagation path is influenced by the structure presence and the structure is left on the footwall side of the new fault trace. In this case, the structure seems not to be threatened by surface displacement from future faulting.
- Zone 3, between zones 2 and 4, where the fault propagation path is influenced by the structure presence but leaves the structure on the hanging wall of the new fault trace. In this case the surface displacement gradient in future faulting could be much more extensive than required in order to threat the structure.
- Zone 4, on the hanging wall but far enough from the free field reverse fault trace, where the structure and the fault have no interaction on each other, and the structure would be not threatened by surface displacement from future faulting.

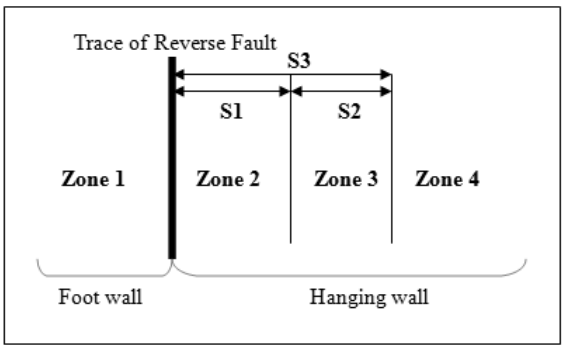

Fig. 18. four distinct fault zones near a reverse fault trace

The widths of zones 2 and 3, denoted by s1 and S2 respectively, depend on various parameters such as the soil's strength and stiffness, the depth of the ground surface to the bedrock, the slip of the bedrock's displacement as well as the foundation's width and its bearing pressure. Proper numerical parametric analysis should be performed in future in order to quantify the weight of each of these mechanical and geometrical parameters.

Considering the above-mentioned aspects of the interesting interaction between the reverse fault propagation pattern and the rigid shallow foundation, encourages one to pay a more careful attention to the widespread concept of the setback. Based on the interaction patterns observed during this study, it seems that it would be neither accurate nor sufficient to define simply an area with boundaries positioned at distances equal to the setback (sb) from the free field fault trace and thereafter forbid placing structures for human occupancy within this area. It seems more reasonable to modify the setback criteria for hanging wall side to: $sb > s1 + s2$. In some certain circumstances, in which the bearing pressure would play a key role, the setback could be even less than s1; i.e. $sb < s1$.

7. Conclusions

This paper presents some clear perspectives of the interaction pattern between surface reverse fault rupture propagation and rigid shallow foundations for relatively small B/H ratio, based on the observations made during a number of 1g physical modeling tests. It is shown that:

1. The foundation's position relative to the free field reverse fault trace as well as its bearing pressure, consist two of the most important parameters that control the interaction of the surface fault rupture propagation and the rigid shallow foundations.
2. Structures would be not threatened by surface displacement from future faulting, if the rigid foundation is located on the footwall of the free field reverse fault trace or it is located far enough from the free field reverse fault trace.
3. Based on fault deviation to the right or left hand side of the footing, the foundation will be located on footwall or hanging wall of the new fault trace. In the former case no threat is foreseen for the foundation but in the latter case the foundation could be threaten.
4. The simple widespread concept of 50 feet setback does not seem to give enough assurance that future faulting would not threaten the existing structures.Based on the intensity of the bearing pressure, the building could be positioned on footwall or hanging wall of the fault leading to different level of vulnerability of foundation and structure.

Nevertheless it is obvious that proper complementary experimental investigations as well as extensive numerical parametric analysis is needed in near future in order to clarify much more and thereupon quantify the reverse fault rupture propagation pattern and its interaction with rigid shallow foundations.

8. Acknowledgment

The authors wish to thank the soil mechanic laboratory staff of the International Institute of Earthquake Engineering and Seismology (IIEES), especially Mr. Shirazian, for their useful helps and efforts.

References

[1] Ulusay, R., O. Aydan and M. Hamada [2001] “The behaviour of structures built on active fault zones: examples from the recent earthquakes of Turkey”, in Seismic Fault-Induced Failures-Possible Remedies for Damage to Urban Facilities, (edited by K. Konagai, University of Tokyo) Japan Soc. Prom. Sci., Japan, pp. 1-26

[2] Bray, J.D. ,2001, "Developing Mitigation Measures for the Hazards Associated with Earthquake Surface Fault Rupture," Seismic Fault-Induced Failures Workshop, Japan

Society for the Promotion of Science, University of Tokyo, Japan, pp. 55-79. [Invited Paper].

[3] Kelson, K.I., Kang, K.-H., Page, W.D., Lee, C.-T., and Cluff, L.S., 2001, Representative styles of deformation along the Chelungpu fault from the 1999 Chi-Chi (Taiwan) earthquake: Geomorphic characteristics and responses of man-made structures: Bulletin of Seismological Society America, v. 91, no. 5, p. 930-952

[4] Faccioli E., Anastasopoulos I., Callerio A., and Gazetas G. , 2008 ,"Case histories of fault-foundation interaction", Bulletin of Earthquake Engineering, 6(4),557–583 DOI10.1007/s10518-008-9089-y

[5] Bray, J. D., R. B. Seed, L. S. Cluff and H. B. Seed [1994]a "Earthquake Fault Rupture Propagation through Soil," Journal of Geotechnical Engineering, ASCE, 120(3), 543-561.

[6] Lazarte, C. A, J. D. Bray, A. M. Johnson and R. E. Lemmer [1994] "Surface Breakage of the 1992 Landers Earthquake and Its Effects on Structures," Bull. Seismol. Soc. Am., Vol. 84, No. 3, pp. 547-561.

[7] Bray, J. D., and K. I. Kelson [2006]. "Observations of Surface Fault Rupture from the 1906 Earthquake in the Context of Current Practice", Earthquake Spectra, Vol. 22, No. S2, pp. S69-S89.

[8] Anastasopoulos, I. & G. Gazetas [2007]. "Foundation-structure systems over a rupturing normal fault: Part I. Observations after the Kocaeli 1999 earthquake", Bull. Earthquake Eng., Vol. 5, No. 5, pp. 253-275.

[9] Jafari M.K., Moosavi S.M., 2008, Lessons to be learned from Surface Fault Ruptures in Iran Earthquakes, Sixth International Conference on Case Histories in Geotechnical Engineering and Symposium in Honor of Professor James K. Mitchell , Arlington, VA (USA)

[10] Cole, D. A., Jr. and Lade, P.V. [1984] "Influence Zones in Alluvium Over Dip-Slip Faults," Journal of Geotechnical Engineering, ASCE, 110(5), 599-615.

[11] Stone, K. J. L. and Wood, D. M. [1992] : Effects of dilatancy and particle size observed in model tests on sand, Soils and Foundations, JSSMFE, Vol. 32, No 4., pp. 43-57.

[12] Tani,K., Ueta K. and N.Onizuka,[1996], Discussion on "Earthquake fault rupture propagation through soil" by J.D.Bray, R.B.Seed, L.S.Cluff and H.B.Seed, J. of Geotechnical Engineering, ASCE, Vol.122, No.1, pp.80-82.

[13] Lee, Jea Woo; Hamada, Masanori; [2005], "An Experimental Study On Earthquake Fault Rupture Propagation Through A Sandy Soil Deposit", Structural Engineering / Earthquake Engineering Vol. 22, No. 1 pp.1s-13s

[14] Bransby, M.F., Davies, M.C.R., El Nahas, A., Nagaoka, S.,2008,Centrifuge modelling of reverse fault-foundation interaction. Bulletin of Earthquake Engineering, 6(4), 607-628

[15] Bray, J. D., R. B. Seed and H. B. Seed [1994]b "Analysis of Earthquake Fault Rupture Propagation through Cohesive Soil," Journal of Geotechnical Engineering, ASCE, 120(3), 562-580.

[16] Anastasopoulos I., Gazetas G., Bransby F., Davies M.C.R., and Nahas El. A. , 2007, "Fault Rupture Propagation through Sand : Finite – Element Analysis and Validation through Centrifuge Experiments", Journal of Geotechnical and Geoenvironmental Engineering, American Society of Civil Engineers , (ASCE), Vol. 133, No 8, pp. 943-958

[17] Berill JB., 1983," Two-dimensional analysis of the effect of fault rupture on buildings with shallow foundations", Soil Dyn Earthquake Eng 2(3):156–160. doi:10.1016/0261-7277(83)90012-8

[18] Yilmaz MT., Paolucci R., 2007,"Earthquake fault rupture–shallow foundation interaction in undrained soils: a simplified analytical approach", Earthquake Eng Struct Dyn ,36(1):101–118

[19] Berberian M. and Yeats R. S., 1999, Patterns of historical earthquake rupture in the Iranian Plateau. Bulletin of Seismological Society of America. v89. 120-139.

[20] Hessami, K., and Jamali, F., 1996. Active Faulting in Iran, Journal of Earthquake Prediction Research, 5 (3), 403-412

[21] PLAXIS [2008], Finite Element Code, Copyright 1997-2008 Plaxis BV.

[22] Shahnazari H. , Salehzadeh H. and Askarinejad A. [2008], "Determination of virtual cohesion in unsaturated sand trenches, using geotechnical centrifuge", International Journal of Civil Engineering, 6(1), 1-9

[23] Baziar M.H., Ghorbani A., Katzenbach R.,2009," Small-Scale Model Test and Three-Dimensional Analysis of Pile-Raft Foundation on Medium-Dense sand", International Journal of Civil Engineering, 7(3), 170-175

[24] Langen HV and Vermeer PA. [1991], "Interface elements for singular plasticity points", International Journal for Numerical and Analytical Methods in Geomechanics, 15, 301-315

[25] Lazarte, C.A. [1996], " The response of earth structures to surface fault rupture," PhD Thesis, University of California at Berkeley